

Mesh Dependency of Stress-based Crossover for Structural Topology Optimization

Cuimin LI, Tomoyuki Hiroyasu, and Mitsunori Miki

Abstract— This paper presents a genetic algorithm (GA) with a stress-based crossover (SX) operator to obtain a solution without “ checkerboard ” patterns for multi-constrained topology optimization problems. SX is based on the element stress. On one hand, smaller mesh size is required to improve the accuracy of structure analysis results. On the other hand, the computation cost of genetic algorithms for structural topology optimization problems (STOPs) increases with a more detailed mesh. Therefore, it is necessary to discuss the mesh dependency of SX for STOPs. Here, the mesh dependency of SX has been investigated through experiments with four different sized meshes. Furthermore, a comparison of evolutionary structural optimization (ESO) and SX is discussed.

I. INTRODUCTION

Major approaches to continuum structure topology optimization include homogenization [1], solid isotropic microstructure with penalization (SIMP) [2], evolutionary structural optimization (ESO) [3] and bi-directional evolutionary structural optimization (BESO) [4], evolutionary computation methods (such as GA, MOGA, and cellular method). Homogenization and SIMP have been applied to solve various engineering problems, and great progress has been made. However, these approaches cannot be applied easily to complicated nonlinear optimization problems. ESO is based on the principle of removing less stressed elements gradually to derive an optimal solution. As an extension of the ESO method, the BESO method allows efficient materials to be added in addition to removal of inefficient materials to remedy the elements deleted in previous processes. However, the rejection and inclusion ratio used in BESO is dependent on a number of other properties [5]. Furthermore, it is questionable whether these approaches can be extended to other design cases, such as multi-physics problems and multiple constrained problems. Recently, GAs for continuum structural topology optimization problems were developed. Bit-strings and bit-arrays are often used as chromosome representations. To solve the disconnected phenomena on geometric solutions, Wang and Tai introduced a graph representation [6]. Another such method is the morphological representation proposed by Tai and Chee [7], [8]. Regardless of the representation used, 2-point crossover is often used as the main operator in GA. However, this type of initial operator does not consider the properties of real problems, and the “ checkerboard-like ” material distribution often occurs. Sigmund and Petersson reviewed numerical instabilities, such as checkerboards, mesh-dependence, and local

minima occurring in applications of topology optimization [9]. They reported that mesh dependence methods reduce “ checkerboard ” pattern because use of a constraint strong enough to make the set compact so that solutions exist, any sequence of admissible designs, such as finite element solutions, has convergent subsequences during compaction. A number of techniques have been adopted to prevent checkerboard-like material distributions, such as smoothing [9], higher-order finite elements [10], [11], and filtering [12]. However, smoothing is based on image processing, which ignores the underlying problem [9]. Moreover, experiments indicated that only higher-order finite element methods with simple GA operators can eliminate the “ checkerboard-like ” material distribution in the solution [13]. Furthermore, it is obvious that using higher-order finite element methods will substantially increase computation cost. Filtering methods, which are variations of image-processing techniques, involve modification of the design sensitivities used in each generation of the algorithm. For filtering methods, the design sensitivities of specific elements depend on a weighted average over the element itself and its eight direct neighbors and are very efficient in removing checkerboards [9]. However, when filtering methods are applied to three-dimensional problems, realization will be very complicated. In this paper, we introduced a stress-based crossover operator [14], [15] in which the connections of neighboring elements are considered during the procedure. Experiments demonstrate that this operator can easily obtain a solution without a checkerboard-like material distribution. GA uses multiple individuals to search the design domain. The finite element analysis for each structure must be performed before fitness evaluation. It is obvious that the computation cost will increase with increases in mesh density. Therefore, it is necessary to discuss the mesh dependency of GA for structure topology optimization. By the bit-string/bit-array representation, it is easy to achieve a variable chromosome length GA for progressive refinement in topology optimization [16].

II. SX TO STOPs

When GAs are applied to STOPs, the design domain is usually divided by a fixed regular mesh to describe the material distributaries. Usually, each mesh is also called an element in the finite element analysis area. Each mesh represents one gene of the chromosome. The distribution of material and voids in the design domain is such that “ 1 ” represents material and “ 0 ” represents void. The chromosome length is equal to the mesh number of the design domain. The straightforward and natural representation

Cuimin LI is with the Graduate School of Engineering, Doshisha University, Kyoto, Japan (phone: 81-774-65-6924; fax: 81+774-65-6780; email: tomo@is.doshisha.ac.jp, licuimin@mikilab.doshisha.ac.jp)

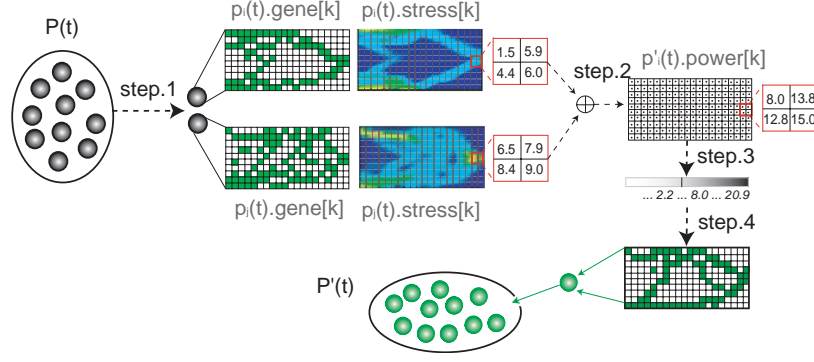


Fig. 1. Stress-base Crossover Operator

method is called a bit-string or bit-array. In this paper the bit-string representation is adopted.

For GAs to structure topology optimization, usually it includes the following procedures. Firstly, the initial population is generated randomly. Then, structure analysis is performed for each individual. Each individual is evaluated according to the fitness function. Selection, crossover, and mutation operations are carried out to generate new offspring. After structure analyses, recombination selection is applied on parent population $P(t)$ and children population $P'(t)$ to generate the next population $P(t+1)$.

By now, simple GA operators for structural topology optimization problems often cause a solution with checkerboard-like material distribution or a solution with disconnected material distribution. One reason for the disconnected phenomenon is that neighbor mesh continuity is not considered correctly. For real problems, the structure properties of the neighboring material, such as stress and stiffness, often change gradually. The ESO method, which can obtain a connected topology, is also based on this principle. To solve this problem, we introduce a stress-based crossover operator in this paper. The following section presents stress-based crossover in detail.

A. Stress-based Crossover Operator

In this section, the procedures of this operator are introduced in detail. The procedures of this operator is also described in Fig. 1. First, the nomenclature used in this operator is explained.

- $P(t) = \{p_i(t) | i \in \{1 \dots n\}\}$ is population of generation t , n is the population size.
- $P'(t)$ is the children population.
- $p_i(t)$ is one individual.
- $p_i(t).weight$ is number of "1" in chromosome.
- $p_i(t).code[k] \in \{0, 1\}$ is genotype of element, where $k \in \{1 \dots N\}$, N is chromosome length.
- $p_i(t).stress[k]$ is stress of element k .
- $p'_i(t).power[k]$ is power of gene k of child individual $p'_i(t)$.

step.1 Randomly select two individuals, p_i, p_j from $P(t)$.

step.2 Add up the stress at each gene of p_i and p_j by formula (1). Naming this value as the power of each gene of child individual $p'(t)$.

$$p'_i(t).power[k] = p_i(t).stress[k] + p_j(t).stress[k], k = 1 \dots N \quad (1)$$

step.3 Sort the power values $p'_i(t).power[k]$ from big to small.

step.4 According to the power value of each gene, the bigger power valued genes will be set "1". Namely, divide the genes into two groups, $U1$ and $U0$. $U1$ is group of the front m genes. $U0$ is group of the last $N - m$ genes. In this study, m is defined by formula (2). Generate a child individual by formula (3).

$$p_i(t+1).weight = \frac{p_i(t).weight + p_j(t).weight}{2} \quad (2)$$

$$p_i(t+1).code[k] = \begin{cases} 1, & \text{if } p_i(t+1).power[k] \in U1 \\ 0, & \text{if } p_i(t+1).power[k] \in U0 \end{cases} \quad (3)$$

Applying these four steps to generate new individuals. After the crossover operation, the mutation operator is applied to each gene of each individual with a small rate. The mutation operator focuses on local search. If the number of '1's in the chromosome decreases, it drives to a lighter topology. On the other hand, increasing the number of 1's in the chromosome may correct infeasible individuals.

III. OBJECTIVE FUNCTION AND FITNESS FUNCTION

A. MBB Beam Problem

The MBB beam with dimensions of 2000×400 (mm) is shown in Fig. 2. The thickness is 10 mm. The design domain is a simple beam supported at its ends, with a downward concentrated load $F = 5.12 \times 10^9$ (N) is applied at the mid-span on the upper frame.

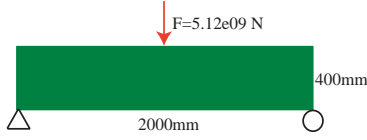


Fig. 2. MBB Beam Problem

$$\begin{aligned} \min. \{f(x_i) = \sum_{i=1}^N x_i\}, x_i \in \{0, 1\} \\ \text{sub. : } Stress_{max} < Stress_{lim}, \\ Displ_{max} < Displ_{lim} \end{aligned} \quad (4)$$

The objective is to minimize the weight of the structure subjected to constrained stress - $Stress_{lim}$ and constrained displacement - $Displ_{lim}$. It can be written as formula (4), where $Stress_{max}$ is maximal stress of structure and $Displ_{max}$ is maximal displacement of structure. For this paper, the constraints are $Stress_{lim} = 3.3 \times 10^7 (N)$ and $Displ_{lim} = 0.33 (mm)$.

B. Mesh Size

For GAs, each structure represents one chromosome. The design domain is divided by hexahedral meshes. Each mesh represents one gene of chromosome. In this paper, the four meshes shown in Fig.3 are used. The size of each mesh is listed in Table I. According to these meshes, the mesh numbers of the design domain are 20×4 , 20×8 , 40×8 , and 40×16 , respectively.

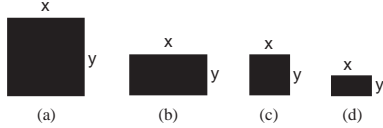


Fig. 3. Mesh Size = (x,y) mm

TABLE I
SIZES OF MESH IN FIG. 3

Index	Mesh Size (x, y) mm
(a)	(100, 100)
(b)	(100, 50)
(c)	(50, 50)
(d)	(50, 25)

C. Fitness Function

The fitness function can be expressed as formula (5) for feasible individuals. In this function, each of the last three items is less than "1". The first item - $weight$ is much bigger than other items so that the fitness function focuses on $weight$. Here, $weight$ is the objective function, $Stress_{max}$ is the maximal stress of an individual, and $perimeter$ is the

outline length of the geometric topology solution.

$$\begin{aligned} fitness(x) = weight + \frac{Stress_{max}}{Stress_{lim}} \\ + \frac{Disp_{max}}{Displ_{lim}} + \frac{perimeter}{4 \times weight} \end{aligned} \quad (5)$$

For infeasible individuals, $weight$ is replaced by a constant, which must be larger than the weight of any feasible individual. In this paper, it is assigned the value of mesh number of the design domain, which means the weight of the full solid material structure.

For GAs to real-world engineering problems, different researchers define different fitness functions to evaluate the individuals, which makes it difficult to decide which solution is the best. Especially for evolutionary computation algorithms to multi-constrained problems, many fitness evaluation approaches have been proposed. According to the above analyses, for GA to multi-constrained problems, different geometric topologies may be searched. Hence, for each mesh size, the experiments are run with the same parameters for six trials.

IV. EXPERIMENTS AND RESULTS

A. GA Parameters

The GA parameters used in this paper are listed in Table II. These parameters are used for all the following experiments. It should be noted that the chromosome length of each experiment is the same as the mesh numbers of the design domain.

TABLE II
GA PARAMETERS

Parameters	Value
PopulationSize	100
ChromosomeLength	mesh number
CrossoverRate	1.0
MutationRate	0.01
TournamentSize	2
EliteNumber	1
Generation	500

B. Experiments of Different Mesh Size

Because of the global search ability of GA and the complexity of structural topology optimization, GAs may derive to different solutions under same parameters. Therefore, we ran multiple trials for each mesh size with the same parameters.

1) *Mesh Size (100, 100) mm*: Geometric solutions of five trials for mesh size (100, 100) mm are shown in Fig. 4. The numerical properties of each solution in Fig. 4 are listed in Table III.

The average weight of six trials is 55%. According to the conceptual definition of structure topology, if the "hole" numbers in the structures are the same they can be taken as one structure topology. Therefore, six trials with mesh size (100, 100) mm obtained the same structural geometric solution.

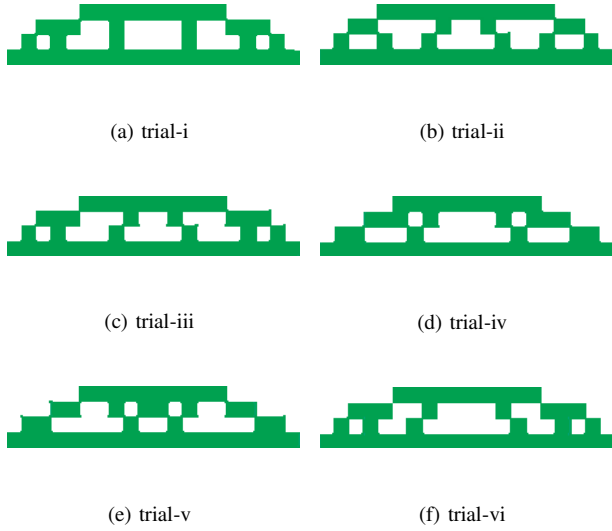


Fig. 4. Results of Mesh Size (100, 100) mm

TABLE III
NUMERICAL RESULTS OF FIG.4

Index	Weight(%)	$Stress_{max}$ (N)	$Disp_{max}$ (mm)
(a)	44 (55%)	1.57143e+07	0.328048
(b)	44 (55%)	1.74756e+07	0.323112
(c)	44 (55%)	2.90405e+07	0.321025
(d)	44 (55%)	1.57678e+07	0.310413
(e)	44 (55%)	1.64023e+07	0.325033
(f)	44 (55%)	1.64459e+07	0.322755

2) *Mesh size (100, 50) mm* : Experiments showed that all geometric solutions of six trials for mesh size (100, 50) mm derive the same topology, as shown in Fig.5. The numerical properties of the solution shown in Fig.5 are listed in Table IV. Hence, the average weight of six trials is 20%.



Fig. 5. Experimental results of mesh size (100, 50) mm

TABLE IV
NUMERICAL RESULTS OF FIG.5

Weight(%)	$Stress_{max}$ (N)	$Disp_{max}$ (mm)
32 (20%)	2.89236e+07	0.31117

3) *Mesh size (50, 50) mm* : Geometric solutions of six trials for mesh size (50, 50) mm are shown in Fig. 6. The numerical properties of each solution shown in Fig. 6 are listed in Table V.

4) *Mesh size (50, 25) mm*: Geometric solutions of six trials for mesh size (50, 25) mm are shown in Fig. 7. The numerical properties of each solution in Fig. 7 are listed in Table VI. The average weight of structure for six trials is 48.1%.

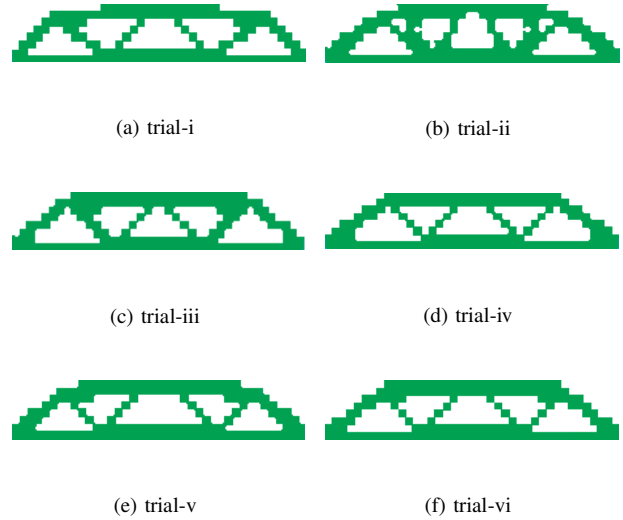


Fig. 6. Results of Mesh Size (50, 50) mm

TABLE V
NUMERICAL RESULT OF FIG.6

Index	Weight(%)	$Stress_{max}$ (N)	$Disp_{max}$ (mm)
(a)	152(47.5%)	2.62234e+07	0.328465
(b)	162(50.6%)	3.14147e+07	0.316905
(c)	160(50.0%)	2.15050e+07	0.316090
(d)	152(47.5%)	2.62118e+07	0.326726
(e)	156(48.75%)	2.95782e+07	0.329426
(f)	154 (48.1%)	2.64110e+07	0.326562

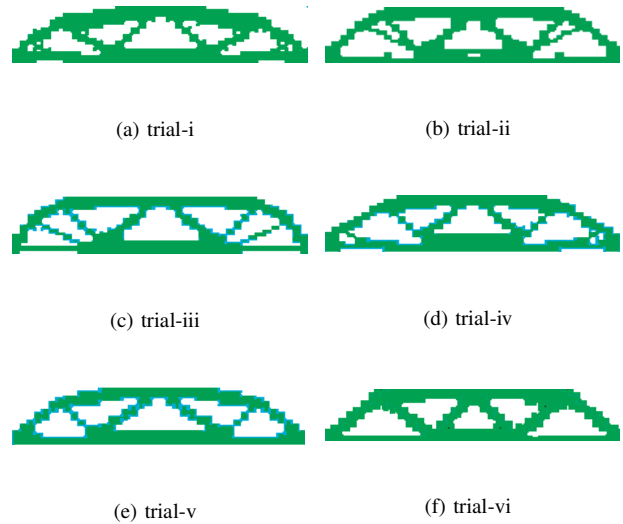


Fig. 7. Results of Mesh Size (50, 25) mm

TABLE VI
NUMERICAL RESULTS OF FIG. 7

Index	Weight(%)	Stress _{max} (N)	Disp _{max} (mm)
(a)	312(48.7%)	3.28484e+07	0.327841
(b)	304(47.5%)	2.78104e+07	0.323325
(c)	304(47.5%)	3.11505e+07	0.324528
(d)	312(48.7%)	3.23893e+07	0.328988
(e)	314(49.1%)	3.07080e+07	0.323759
(f)	302(47.2%)	2.56965e+07	0.325971

V. RESULTS AND DISCUSSION

A. Resulting topology of mesh size (100, 50)

SX experiments showed that with a mesh size of (100, 50) mm, the geometric results were very different from the solutions obtained with other meshes for both SX and ESO. To explore these observations further, we first discuss FEA results with regard to mesh size.

1) *Discussion of FEA results to mesh size:* The topologies shown in Fig. 8 and Fig. 9 are re-meshed with size (50, 50) mm and the topologies are re-analyzed. The numerical properties are listed in Table VII and Table VIII.



Fig. 8. solution with mesh (100, 100) mm

TABLE VII
NUMERICAL PROPERTIES OF TOPOLOGY IN FIG. 8

Mesh Size (mm)	Stress _{max} (N)	Disp _{max} (mm)
(100,100)	1.57143e+07	0.328048
(50, 50)	3.17001e+07	0.390245



Fig. 9. solution with mesh size (100, 100) mm

From the comparisons of the numerical results in Table VII and Table VIII, we can conclude that the mesh size affects the finite element analysis results. Overall, variation in stress and variation in displacement are the same. The difference between mesh size (100, 100) mm and mesh size (50, 50) mm is not large. However, it should be noted that this problem is caused by finite element analysis and not by the topology optimization algorithms.

2) *Discussion of mesh size (100, 50):* Similarly, the topology in Fig. 5 is re-analyzed with a mesh of (50, 50) mm. The topology properties are listed in Table IX.

The comparison showed that for mesh size (100, 50) mm and mesh size (50, 50) mm, the variations of structure properties in stress and displacement are significant. Especially for displacement, maximal displacement with mesh size (50, 50) is more than 300 times bigger than that with mesh size

TABLE VIII
NUMERICAL PROPERTIES OF TOPOLOGY IN FIG. 9

Mesh size (mm)	Stress _{max} (N)	Disp _{max} (mm)
(100,100)	1.74756e+07	0.323112
(50,50)	1.89271e+07	0.376026

TABLE IX
NUMERICAL PROPERTIES OF FIG. 5

Mesh Size	Stress _{max} (N)	Disp _{max} (mm)
(100,50)	2.89236e+07	0.31117
(50,50)	1.43263e+08	97.9899

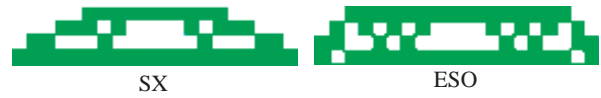
(100, 50). According to the preceding section discussion we know that structure properties variations of good topology are not large. Therefore, it indicates that the solution with mesh size (100, 50) is an ill-topology. This problem also occurred for the ESO approach. Hence, we conclude that a cube mesh is better than non-cube mesh.

Nevertheless, with mesh (50, 25), which is of the same type as mesh (100, 50) but a different size, the geometric solution of SX shown in Fig. 7 is similar with geometric solution with cube mesh shown in Fig. 6. This observation indicates that with the decreasing of mesh size there is no difference for cube mesh and non-cube mesh.

B. Comparison of SX with ESO

ESO, as an effective approach to STOPS, has been widely used to solve various engineering problems. This method is also based on stress. Therefore, to further study the mesh dependency of SX, a comparison of ESO and SX is carried out. For ESO to constrained problems, evolution will stop once the result violates the constraints.

The best solution of SX for different mesh sizes and ESO results are shown in Fig. 10.



(a) solutions with mesh size (100, 100) mm



(b) solutions with mesh size (50, 50) mm



(c) solutions with mesh size (50, 25) mm

Fig. 10. Results Comparison of SX and ESO

Accordingly, the numerical properties of each solution with each mesh size are listed in Table X.

TABLE X
NUMERICAL PROPERTIES OF SOLUTIONS

Index	Weight(%)	Stress _{max} (N)	Disp _{max} (mm)
(a)-SX	44 (55%)	1.57678e+07	0.310413
(a)-ESO	50 (62.5%)	1.58790e+07	0.271756
(b)-SX	152(47.5%)	2.62118e+07	0.326726
(b)-ESO	154(48.1%)	3.14594e+07	0.327699
(c)-SX	302(47.2%)	2.56965e+07	0.325971
(c)-ESO	322(50.3%)	3.29281e+07	0.328190

The geometric results comparison of SX and ESO shown in Fig. 10 demonstrates SX searched out the same topology with different mesh sizes. The numerical results indicate that with the decreasing mesh size, the structure weight is smaller and smaller. In contrast, for ESO, different mesh size derives to solutions with different geometric topologies. Furthermore, the objective function - *weight* does not decrease with decreasing mesh size. Moreover, with smaller mesh size, the solution becomes complex.

Furthermore, the SX results demonstrate that a certain mesh size is detail enough to obtain a satisfactory solution, and subsequent reductions in the mesh size do nothing to derive a more optimal solution. This can also be seen in Fig. 11, which shows the solution weight of SX with different mesh sizes. For this MBB beam problem, geometric topology with mesh size (100, 100) mm is approximate with geometric topology with mesh size (50, 50) mm.

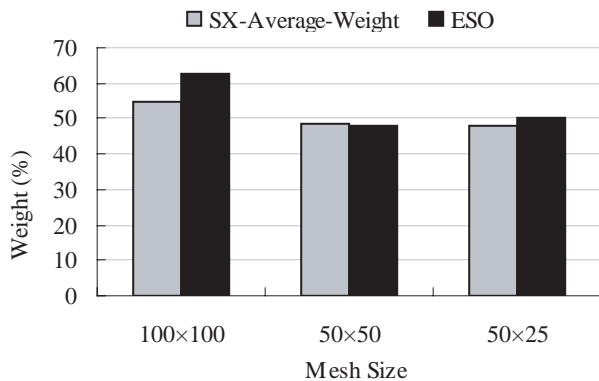


Fig. 11. Solution Weight Comparison

VI. CONCLUSION

GAs, as global search algorithms, have been applied to solve various types of real-world problems because of their flexibility for complicated problems. However, there is no way to avoid the long computation times for individual evaluations. Especially, when GAs are applied to solve STOPS, the finite element analysis time for each individual is much longer. From the viewpoint of computation cost reduction, it is necessary to discuss the mesh dependency of GA.

In this paper, a stress-based crossover operator was introduced to suppress the “ checkerboard-like ” material distribution that is often seen with simple GAs. four different meshes were adopted in experiments to examine the mesh dependency of SX. A comparison of ESO and SX was also performed.

The experiments yielded the following conclusions. First, FEA solution accuracy is dependent on mesh size. However, for good topology, the differences in structure properties for different mesh sizes are not significant. Second, a cube mesh is better than other types of mesh for obtaining a good solution. With a cube mesh, a more detailed mesh size allows the derivation of a more optimal solution. However, the differences become smaller with decreasing mesh size. Thus, there is a threshold mesh size that is sufficient for topology optimization.

REFERENCES

- [1] Bendsoe, M.P. and Kikuchi, N., "Generating optimal topologies in structural design using a homogenization method," *Comput. Methods. Appl. Mech. Engre.*, Vol.71, pp.197-224, 1988.
- [2] G. I. N. Rozvany, M. Zhou, T. Birker, "Generalized shape optimization without homogenization," *Strutural Optimization*. Vol.4, pp.250-254, 1992.
- [3] Xie, Y. M., Steven, G. P. "Shape and Layout Optimization via an Evolutionary Procedure," *Proc. International Conference on Computational Engineering Science*, Hong Kong, 1992.
- [4] O. M. Querin, G. P. Steven and Y. M. Xie, "Evolutionary Structural Optimization (ESO) Using a Bidirectional Algorithm," *Engineering Computations*, Vol.15(8), pp.1031-1048, 1998.
- [5] V. Young, O. M. Querin, and G. P. Steven, "3D and multiple load case bi-directional evolutionary structural optimization (BESO)," *Structural Optimization*, Vol.18, pp.183-192, 1999.
- [6] S. Y. Wang and K. Tai, "Graph representation for structural topology optimization using genetic algorithms," *Computers and Structures*, Vol.82, pp.1609-1622, 2004.
- [7] Tai K. and Chee TH., "Genetic algorithm with structural morphology representation for topology design optimization," *Proc. 2nd international conference on mechanics in design*, Nottingham, UK, pp.827-836, 1998.
- [8] Tai K. and Chee TH., "Design of structures and compliant mechanisms by evolutionary optimization of morphological representations topology," *ASME Journal, Mechanism Design*, Vol.122(4), pp.560-566, 2000.
- [9] O. Sigmund and J. Petersson, " Numerical instabilities in topology optimization: A survey on procedures dealing with checkerboards, mesh-dependencies and local minima ", *Structural Optimization*, Vol.16, pp.68-75, 1998.
- [10] Diaz, A. R. and Sigmund O., " Checkerboard patterns in layout optimization ", *Structural Optimization*, Vol.10, pp.40-45, 1995.
- [11] Jog C. S and Haber R. B. " Stability of finite element models for distributed-parameter optimization and topology design ", *Comp. Meth. Appl. Mech. Engng.*, Vol.130, pp.203-226, 1996.
- [12] Sigmund, O., *Design of material structures using topology optimization. Ph.D. Thesis*, Department of Solid Mechanics, Technical University of Denmark, 1994.
- [13] Chapman, C. D, Saitou, K., and Jakiela, M. J., " Genetic Algorithms as an Approach to Configuration and Topology Design ", *ASME Journal of Mechanical Design*, Vol.116, No.4, pp.1005-12, 1994.
- [14] Cuimin Li, Tomoyuki Hiroyasu, and Mitsunori Miki, " Stress-based crossover operator for structural topology optimization ", JSME, submitted.
- [15] Cuimin Li, Tomoyuki Hiroyasu, and Mitsunori Miki, " an improved stress-based GA for multi-constrained topology optimization ", *Proceedings of APCOM '07-EPMEESC XI*. Kyoto, Japan, 2007.
- [16] I. Y. Kim and O. L. de Weck, " Variable chromosome length genetic algorithm for progressive refinement in topology optimization ", *Struct. Multidisc. Optim*, 2005.